

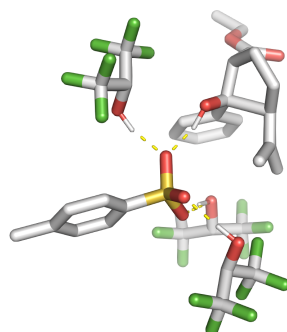
Hydrogen Bonding Networks Enable Brønsted Acid-Catalyzed Carbonyl-Olefin Metathesis

Tuong Anh To,[†] Chao Pei,[§] Rene M. Koenigs,^{*§} Thanh Vinh Nguyen^{*†}

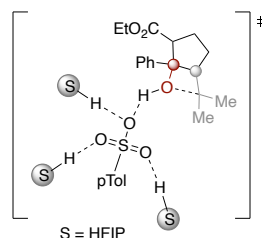
[†]*School of Chemistry, University of New South Wales, Sydney, NSW 2052, Australia*

[§]*Institute of Organic Chemistry, RWTH Aachen, Aachen D52074, Germany*

Catalyst activation by hydrogen bonds



Hydrogen bond complex of pTSA and HFIP and substrate in carbonyl olefin metathesis reactions



- Hydrogen bond network between catalyst and multiple molecules of HFIP
- Increased catalytic efficiency of Brønsted acid catalyst and stabilize reaction intermediates
- Mechanism of action revealed by experimental and DFT studies

Abstract: Synthetic chemists have learned to mimic nature in using hydrogen bonds and other weak interactions to dictate the spatial arrangement of reaction substrates and to stabilize transition states to enable highly efficient and selective reactions. The activation of a catalyst molecule itself by hydrogen bonding networks, in order to enhance its catalytic activity to achieve a desired reaction outcome, is less explored in organic synthesis, despite being a commonly found phenomenon in nature. Herein, we show our investigation into this underexplored area by studying the promotion of carbonyl-olefin metathesis reactions by hydrogen bonding-assisted Brønsted acid catalysis, using hexafluoroisopropanol (HFIP) solvent in combination with *para*-toluenesulfonic acid (pTSA). Our experimental and computational mechanistic studies reveal not only an interesting role of HFIP solvent in assisting pTSA Brønsted acid catalyst, but also insightful knowledge about the current limitations of the carbonyl-olefin metathesis reaction.

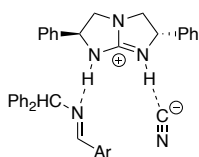
19 Introduction

20 Weak non-covalent interactions take up an essential role in chemistry and biology and form the basis
21 for the assembly of complex supramolecular structures in natural and artificial systems.¹ Among them,
22 the hydrogen bond is of unique importance and indispensable for the formation of entities essential
23 for living, such as proteins or nucleic acids.² Chemists often mimic nature in using hydrogen bonds to
24 dictate the spatial arrangement of individual molecules in supramolecular assemblies³ or to stabilize
25 transition states in catalysis to enable highly efficient and selective reactions.⁴ One of the longest
26 standing paradigms in catalysis lies within the activation of reaction substrates with hydrogen-bonding
27 catalysts, which also are small organic molecules themselves.⁵ Numerous hydrogen-bonding motifs
28 have been reported to date and the Corey, Schreiner or Takemoto catalysts (Scheme 1a) represent a
29 few versatile and well-explored examples of such systems. Nonetheless, the activation of a catalyst
30 molecule itself by hydrogen bonding is relatively less explored in organic synthesis, despite being a
31 common occurrence in biological chemistry.^{2, 4c}

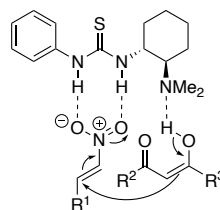
32 We believe that this strategy would be useful in frequently encountered synthetic scenarios where
33 highly reactive catalysts are not only efficient for the desired chemical transformation but also
34 promote unwanted side-reactions at the same time.⁶ By employing a moderately or poorly active
35 catalyst to ensure better selectivity, and enhancing its efficacy by hydrogen bonding interactions, the
36 overall outcome of the catalytic reaction can be improved. For this purpose, it is ideal for the reaction
37 solvent to also act as the required hydrogen-bonding molecules.^{4b} While there are many solvents
38 capable of forming hydrogen bonds, with water being the one in biological systems, perfluorinated
39 alcohols such as HFIP are attractive options for organic synthesis.⁷ HFIP has been known to mediate a
40 wide range of reactions as a highly ionizing solvent with excellent hydrogen bonding capability, yet, its
41 unique role in catalysis remains poorly understood.⁸ Simple and mildly Brønsted acidic catalysts with
42 multiple hydrogen bond acceptor groups, such as carboxylic acids or sulfonic acids, could become
43 suitable models to further explore the concept of catalyst activation by hydrogen-bonding networks.

a) Substrate activation by hydrogen bonds

Corey catalyst
Monofunctional catalyst



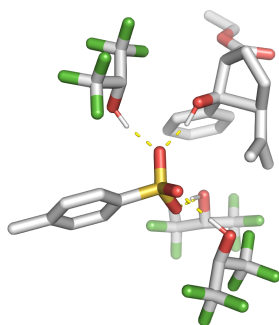
Takemoto catalyst
Bifunctional thiourea catalyst



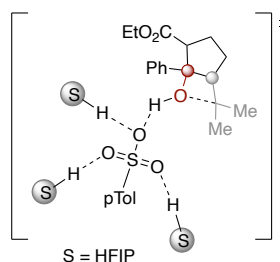
hydrogen bond activation in organocatalysis

- Substrate activation via hydrogen bonds
- Preorganization of substrates via hydrogen bonds

b) This work: Catalyst activation by hydrogen bonds



Hydrogen bond complex of
pTSA and HFIP and substrate in
carbonyl olefin metathesis reactions



- Hydrogen bond network between catalyst and multiple molecules of HFIP
- Increased catalytic efficiency of Brønsted acid catalyst

44

45

46

47

48

49

50

51

52

53

54

55

56

57

58

59

60

61

62

Scheme 1. Hydrogen-bonding complexation with solvent activates Brønsted acid catalysts for the promotion of otherwise challenging chemical transformation.

To study such novel catalyst systems, we embarked on the investigation of their efficiency on the carbonyl olefin metathesis (COM) reaction.⁹ The COM reaction has been identified as an attractive replacement to overcome challenges in traditional approaches for the olefination of carbonyl groups, such as pre-functionalization of substrates, reagent synthesis, or the separation of by-products from reaction mixtures.¹⁰ The majority of approaches towards COM reactions are based on Lewis acid catalysts,¹¹ ranging from transition metal salts such as FeCl₃ first reported by Schindler *et al.*^{9c, 12} and Li *et al.*^{9d} and subsequently salts of Ga(III) by Schindler¹³ and Bour,^{9f} AuCl₃ by Lin *et al.*¹⁴ or bimetallic systems such as AlCl₃/AgSF₆ and AlCl₃/AgSF₆ by Schindler¹⁵. Further, more specialized approaches harness the reactivity of hydrazines as organocatalysts as reported by the Lambert group^{9a, 16} and a special photocatalytic strategy by the Glorius group.^{9e} There have also been notable applications of metal-free Lewis acids in promoting COM reactions such as the tritylium catalysts by Franzén and co-workers^{9b, 17} as well as tropylium salts¹⁸ and iodonium ion¹⁹ reported by our Nguyen group. Silylium or phosphonium-based Lewis acids also showed potential catalytic activity for COM reactions.²⁰ Despite recent advances in COM reactions with various Lewis acid catalysts,¹⁰ the field is still in its infancy and a generalized approach towards Brønsted acid-catalyzed COM reactions remains elusive. Up to this

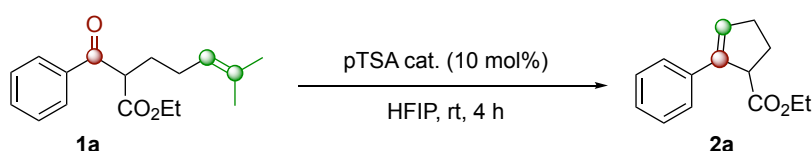
date, there have been only two reports on efficient Brønsted acid catalyzed COM reactions, with both of them employing elegant but very specially designed systems using fixation of the acid catalyst in a supramolecular capsule by the Tiefenbacher group²¹ or within a fixed-bed in continuous flow system by Layva-Pérez and co-workers.²² Simple generalized methods towards COM reactions that can operate homogeneously in bulk solvent have not been reported thus far. Furthermore, the COM reaction is even more suitable for the investigation of our catalysis concept (Scheme 1b), considering the fact that previous attempts to use superacidic catalysts such as triflic acid to catalyze COM reaction often led to unsatisfactory or unwanted outcomes.²³

71

72 Reaction optimization and mechanistic investigations

To probe our hypothesis on hydrogen bond network-assisted, Brønsted acid-catalyzed COM reactions, we studied the influence of solvent on the reaction substrate **1a** using pTSA as a simple readily available Brønsted acid catalyst. Pleasingly, the reaction worked optimally with 10 mol% of pTSA catalyst in 100 μ L HFIP for the 0.2 mmol scale reaction, giving the product **2a** in 80% yield after 4 hours at ambient temperature (entry 1, Table 1).²⁴ Solvents such as 1,2-dichloroethane (DCE), *i*PrOH or linear fluorinated alcohols, which are weaker hydrogen-bonding agents than HFIP, proved to be inefficient (entries 2-6, Table 1). ¹H NMR studies on the perturbation of the pTSA acidic proton signal in the presence of a varying amount of HFIP showed clear evidence of such a hydrogen-bonding network, and this effect was stronger with HFIP than *i*PrOH or TFE (see page S4-S7 in the experimental SI for further details). The respective ¹H NMR studies on the interaction of HFIP with substrate **1a** showed no evidence on potential solvent-substrate interaction (see page S8 in the experimental SI).

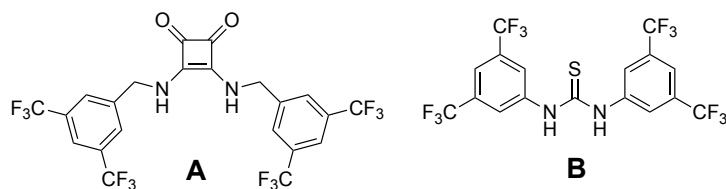
84 **Table 1.** Optimization of the HFIP-promoted Brønsted acid-catalyzed COM.



85

Entry ^[a]	Variations from optimal conditions ^[b]	Yield ^[c]
1	None (HFIP = 100 μ L)	80%
2	Neat	n.p.
3	DCE instead of HFIP	n.p.
4	<i>i</i> PrOH instead of HFIP	n.p.
5	TFE (CF ₃ CH ₂ OH) instead of HFIP	15%
6	CF ₃ CF ₂ CH ₂ OH instead of HFIP	n.p.

7 Catalyst **A** or **B** (10 mol%) instead of pTSA, in HFIP n.p.



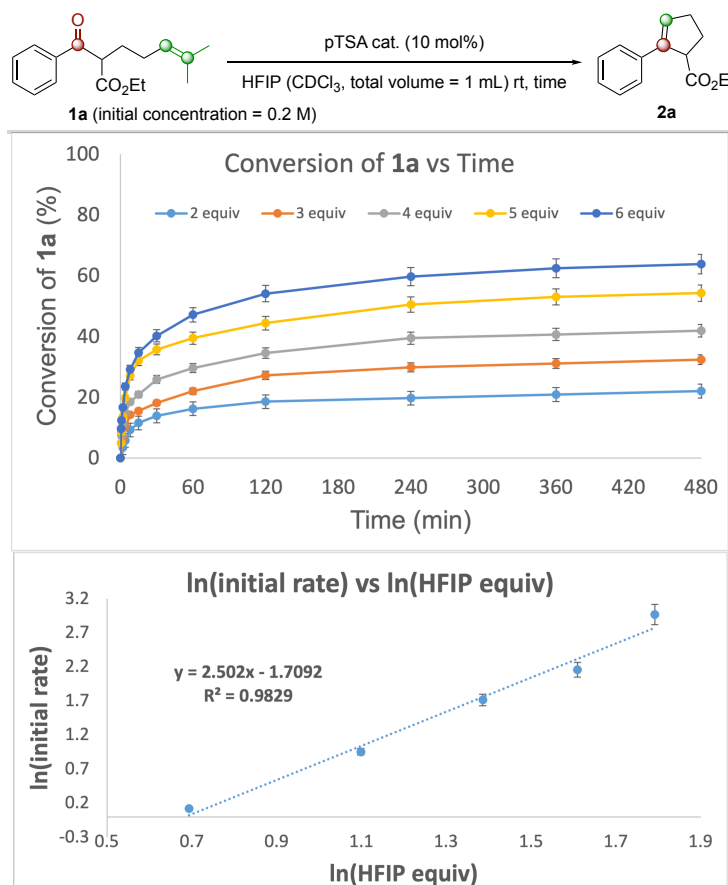
8	pTSA and catalyst A or B (10 mol%, instead of HFIP), in DCE	n.p.
9	Absence of pTSA	n.p.
10	pTSA (5 mol%)	73%
11	TfOH (10 mol%) instead of pTSA, in HFIP	66%
12	TfOH (10 mol%) instead of pTSA, in DCE instead of HFIP	36%
13	HCl (10 mol%) instead of pTSA, in HFIP	traces
14	TFA (10 mol%) instead of pTSA, in HFIP	traces
15	HFIP (50 μ L)	56%
16	HFIP (75 μ L)	62%
17	HFIP (200 μ L)	80%

[a] Reaction conditions: **1a** (0.2 mmol), pTSA (10 mol%), HFIP (100 μ L) at rt for 4 h. [b] For further details on optimization studies, see pages S9-S10 in the experimental SI. [c] Yield based on ^1H NMR integration using methyl benzoate as an internal standard, n.p. = no product.

Furthermore, the use of a squaramide or a thiourea catalyst as hydrogen-bonding donors did not lead to any productive outcomes either (entries 7-8), thus demonstrating the importance of HFIP and the formation of a strong hydrogen bond network to enhance catalytic efficiency of pTSA and improve the efficiency of the COM reaction. In the absence of catalyst, no reaction was observed (entry 9) and lower catalyst loading was detrimental to the reaction efficiency (entry 10). pTSA was superior to a range of other Brønsted acids, including strong acids such as triflic acid (TfOH) as well as HCl or trifluoroacetic acid (entries 11-14), highlighting the special role of HFIP in mediating the COM reaction with a mildly acidic catalyst. It should be noted here again that previous attempts using triflic acid to catalyze COM reactions often led to different or unsatisfactory outcomes,²³ especially in other solvent than HFIP as evidenced by entry 14 (Table 1) Reducing the amount of HFIP led to lower efficiencies while using more HFIP resulted in comparable reaction outcomes (entries 15-17). Overall, the optimal conditions developed here are milder and more practical than previous reports on other Brønsted acid catalyzed COM systems, which used more complicated reaction setups, elevated temperatures and longer reaction times.²¹⁻²²

For further understanding of the reaction mechanism and the role of HFIP and the hydrogen bond network on the reaction, we carried out a series of kinetic studies with substrate **1a** and 5 mol% of pTSA in varying amount of HFIP from 2 to 6 equivalents with respect to **1a** in CDCl_3 (Figure 1). The

conversion of **1a** was monitored by ^1H NMR spectroscopy over time (see pages S11-S12 in the experimental SI for more details). The kinetic data for initial reactions rates after $\sim 10\%$ conversions was analyzed and showed that the reaction order in HFIP was ~ 2.5 (Figure 1), which suggested that only a small number of HFIP solvent molecules were directly involved in the rate determining step of the COM reaction under investigation.



112

113 **Figure 1.** Kinetic studies of the conversion of **1a** to product **2a** with different amounts of HFIP (See pages S11-S12 in the
114 experimental SI for more details).

115

116 To understand experimental reaction kinetics and to rationalize the influence of HFIP on the reaction
117 mechanism, we next embarked on computational studies on the pTSA-catalyzed reaction of **1a**
118 (Scheme 2). First, we examined an implicit solvent model for HFIP²⁵ that does not allow for interaction
119 of solvent molecules with substrate and/or catalyst (Scheme 2a, grey energy profile). Second, we used
120 a combination of explicit solvent molecules and an additional implicit solvent model. For this, we added
121 varying amounts of explicit molecules of HFIP to the calculation to account for the formation and
122 influence of a hydrogen bond network between solvent molecules and catalyst (Scheme 2a, dark blue
123 energy profile).

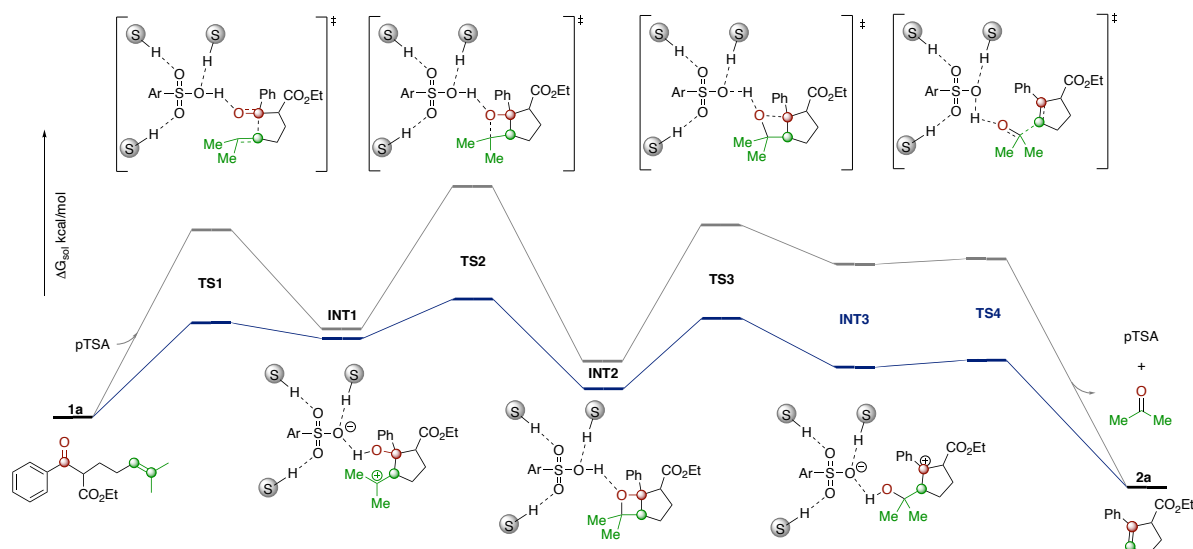
Disregarding of the solvent model used, the calculations show that this COM reaction proceeds via the same elementary reactions steps and initiates via an intramolecular C-C bond formation reaction, followed by oxetane formation, ring opening and elimination reaction to provide olefin product **2a**. Each of these four elementary reaction steps is catalyzed by pTSA, i.e. (i) activation of the carbonyl group in the C-C bond formation step, (ii) and (iii) hydrogen bond interactions during ring-closing and ring-opening of the oxetane and (iv) activation of the carbonyl group that leads to cleavage of the acetone by-product and release of the COM product, respectively.

While the reaction pathway is not altered by the introduction of the hydrogen bond network and with/without the hydrogen bond network the oxetane ring formation remains the rate-determining step. The hydrogen bond network has however a significant influence on the activation free energy along the path of the COM reaction (Scheme 2a, grey vs. blue profile). For instance, the barrier of the initial C-C bond formation is reduced from 23.9 to 12.9 kcal/mol in the presence of 3 molecules of HFIP (Scheme 2a, **TS1**). Similarly, the introduction of 3 molecules of HFIP leads to a significant reduction of the activation free energy of the oxetane formation, which was identified as rate-determining step with an activation free energy of 30.2 kcal/mol without HFIP and 14.8 kcal/mol in the presence of 3 molecules of HFIP, respectively. In the second stage of the reaction, the oxetane intermediate **INT2** is ring-opened in the presence of the pTSA catalyst. The introduction of additional molecules of HFIP similarly leads to a marked reduction of the activation free energies, e.g. from 25.3 to 13.9 kcal/mol for the formation of the carbocation intermediate **INT3** upon introduction of three explicit molecules of HFIP. Thus, the formation of a hydrogen bond network of **1a**, pTSA and three molecules of HFIP leads to a significant lowering of the activation free energy and renders the room temperature COM reactions with simple Brønsted acids possible. These results agree well with our experimental kinetic studies (Figure 1).

In the course of this analysis, we also examined the potential solvent-substrate interaction of HFIP with other Lewis-basic sites of **1a**. Although, such HFIP-substrate interactions were found possible, their influence on the course of the reaction was not taken further into account. These very weak HFIP-substrate interactions are in equilibrium with unbound HFIP and free substrate molecules (see page S8 in the experimental SI for HFIP-substrate complexation study) and thus would not affect the course of the reaction. For example, the hydrogen-bonding of **1a** with the pTSA-HFIP₃ catalyst is favored by 1.4 kcal/mol over the non-bonding situation. The respective interaction for acetone is favored by 1.5 kcal/mol - thus an equilibrium between bound and free catalyst will be present in solution and can drive the reaction to product formation (please see the computational SI for further details).

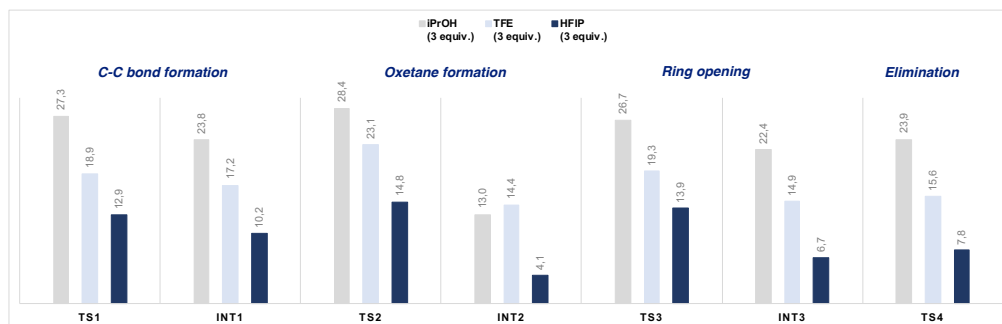
a) Influence of hydrogen bond network on the reaction profile of the COM reaction

Evaluation of implicit solvent model for HFIP (grey) and a combined explicit-implicit solvent model (dark blue). Structures presented are representative for the combined explicit-implicit solvent model



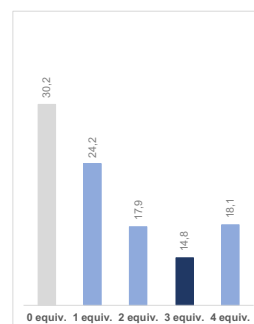
b) Calculated free energy for transition states and intermediates

Evaluation of the influence of three different alcohols.



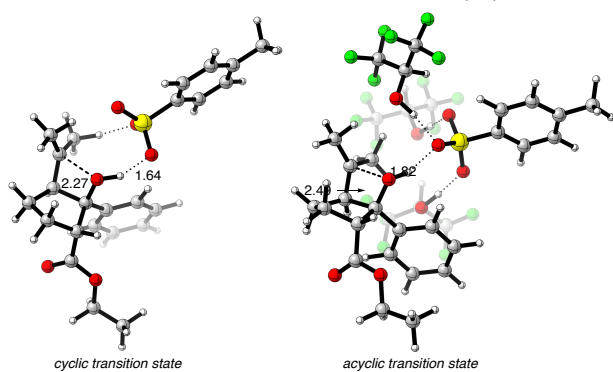
c) Influence of the stoichiometry

Influence of number of explicit HFIP molecules



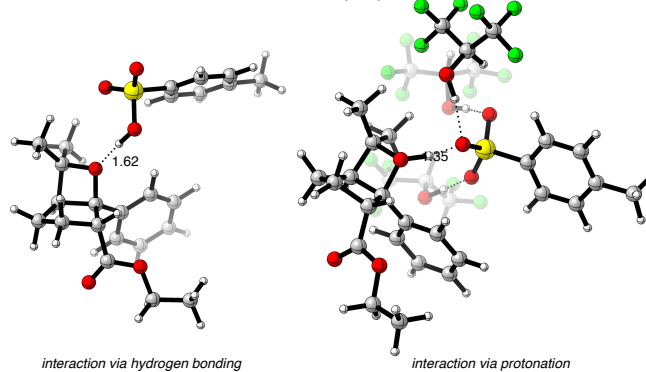
d) Comparison of a selected transition state

Transition state for oxetane formation (TS2)



e) Comparison of a selected intermediate

Oxetane Intermediate (INT2)



Scheme 2. Theoretical calculations on the pTSA-catalyzed COM reaction and the influence of HFIP hydrogen bond networks. Level of theory: B3LYP-D3BJ/def2-tzvp (SMD = HFIP)//B3LYP/def2-svp.

Next, we performed a closer examination of the influence of the hydrogen bond network with different alcohol solvents on the activation of the pTSA catalyst (Scheme 2b). First, we examined *i*PrOH as a close analogue of HFIP to model the influence of a weak hydrogen bond donor (Scheme 2b, grey). In this case relatively high activation free energies were observed, which are comparable to calculations

with an implicit solvent (cf. Scheme 2a). The activation free energy of the rate-determining step was calculated with 28.4 kcal/mol, which is too high to proceed at room temperature with reasonable efficiency. Next, we examined trifluoroethanol as a model for an increased ability to form hydrogen bond networks (Scheme 2b, light blue). In comparison to *i*PrOH, the hydrogen bond network of solvent and catalyst results in a significant reduction of the activation free energy of all transition states. However, only in the case of the strong hydrogen bond donor HFIP (Scheme 2a and 2b, dark blue), the activation free energies for all reaction steps are significantly reduced to enable for efficient COM reaction. Further calculations concerned the analysis of the influence of the stoichiometry of HFIP and catalyst. This analysis reveals that three molecules of HFIP form an optimal hydrogen bond network and allow for the COM reaction to proceed under mild conditions (Scheme 2c), which can be attributed to the presence of three oxygen atoms in pTSA that are required for hydrogen bonding to three molecules of HFIP (Scheme 2d,e). These calculations now show that HFIP engages in the formation of hydrogen bonding interactions with the pTSA catalyst that results in an encapsulation of the catalyst within a hydrogen bond network. This hydrogen bond network thus alters properties of the pTSA catalyst and consequently the transition state energies for each step.

Substrate Scope and Further Applications

The optimized conditions developed in Table 1 were then applied to a range of intramolecular COM substrates (Scheme 3b). β -Substituted ketoester substrates reacted smoothly to form their corresponding cyclopentene products in moderate to high yields (**2a-i**). For some substrates, the isomerized cyclopentenones were obtained as major products (**2'e** and **2'h**), which was expected in this Brønsted acidic environment. Five-membered *N*-heterocyclic products could also be formed by this method in good to high yields, although the reactions on non β -substituted systems (**2l-m**) were less efficient than those of α -substituted ones (**2j-k**). The reaction worked particularly well to form indene derivatives (**2n-q** and **2'r**), which can be attributed to the stability of the conjugate indene ring that formed (Scheme 3). Similarly, a range of naphthalene products (**2s-u**) could be efficiently synthesized using our developed conditions. There were also competing carbonyl-ene side processes in these reactions. The application of these conditions to the formation of six-membered carbocyclic or *N*-heterocyclic products only led to moderate reaction outcomes (**2v-y**, Scheme 3b).

As discussed earlier, the directed Brønsted acid catalyzed COM reaction in homogeneous conditions is often problematic in that several side processes such as carbonyl-ene, Prins or interrupted carbonyl-olefin metathesis reactions can occur.²³ As our pTSA/HFIP catalytic system marked the first time COM reactions can be carried out in this manner without much of those issues, we would like to expand the

work to investigate the scope of its catalytic activity on analogous cyclization reactions. We decided to select a series of aromatic ketones with an unsaturated side chain (**1**, **3**, **5**, **7**, **9** Scheme 3) and subjected them to the pTSA/HFIP catalytic conditions. The α,β -unsaturated ketone substrates in Scheme 3a were based on Schindler's interrupted COM reaction substrates.^{23a} They have unsaturated side chains with one more carbon than the COM α,β -unsaturated ketone substrates in Scheme 3b. The α,β -unsaturated ketone substrates in Scheme 3c can be considered one CH₂ truncated versions of the COM substrates. The alkenyl and alkynyl keto substrates in Scheme 3d and 3e bear slightly different unsaturated side chains but can be considered synthetic equivalents of the ones in Scheme 3c.

Most of these tested substrates cyclized under our pTSA/HFIP catalytic conditions to give the corresponding products (**2**, **4**, **6**, **8**, Scheme 3) in moderate to high yields within four hours at ambient temperature. Some cyclization processes required to be carried out at 50 °C to afford satisfactory outcomes, as indicated by product yields in parentheses. It is interesting to see that electron-donating substituent such as OMe or electron-withdrawing substituent such as NO₂ can have completely opposite effects on the outcomes of these *6-endo-trig* (Scheme 3c), *5-exo-dig* (Scheme 3d) and *5-exo-trig* (Scheme 3e) cyclization reactions.

When there was an aromatic substituent at the alpha position, the *6-endo-trig* cyclization was not the only predominant reaction pathway (Scheme 3c, product **6e/6e'**). The substrate could also cyclize in a Friedel-Crafts alkylation fashion to form tetrahydronaphthalene product **6e'**, which became the single major product at elevated temperature. This reaction pathway²⁶ is directly relevant to the formation of products **4** in Scheme 3a, where presumably the carbocation intermediate from a COM process also underwent Friedel-Crafts alkylation reaction onto the adjacent aromatic ring to form the tricyclic system.^{23a} Such interrupted COM reaction is possible for this type of substrate but not the typical COM substrate (Scheme 3b), which can be attributed to the conformational arrangement of the initially formed six-membered ring. The efficiency of the interrupted COM reaction mediated by our pTSA/HFIP, albeit not fully optimized, was slightly lower than that of the earlier study with TfOH catalyst by Schindler and co-workers.^{23a} It posed the question of how different does HFIP make those pTSA-catalyzed reactions in Scheme 3 in comparison to a normal organic solvent. Furthermore, would the super Brønsted acidic TfOH overcome the need for the '*magical effect*' of HFIP to efficiently promote those cyclization reactions in a normal organic solvent?

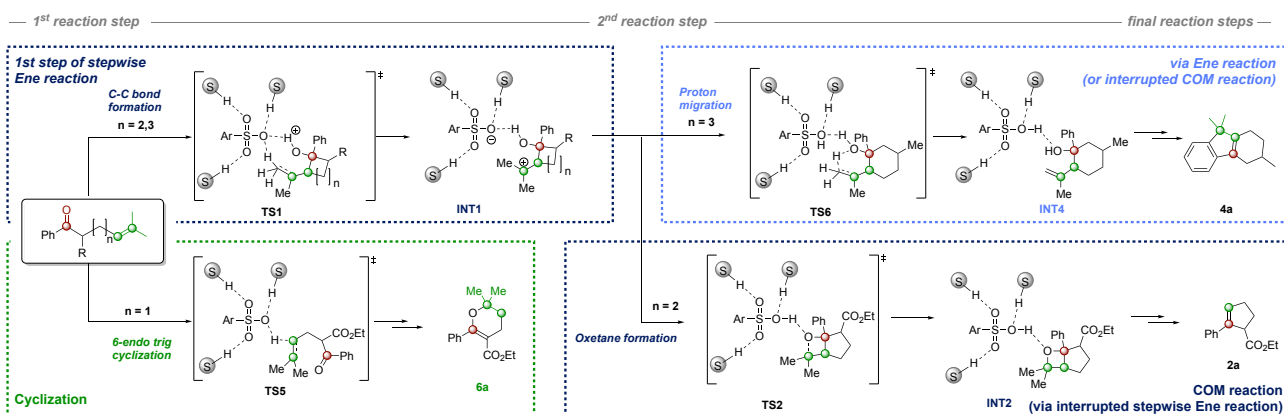
232 Thus, we decided to carry out a comparative study where we performed two of each type of the 6-
233 *endo-trig* cyclization, the COM reactions and the interrupted COM reactions in different sets of
234 conditions with pTSA/HFIP and TfOH/DCE (Table 2, for further details on these studies and also the
235 reaction performances on the 5-*exo-trig*, 5-*exo-dig* cyclizations, see page S69 in the experimental SI).
236 Interestingly, we observed clear differences in reaction efficiency. pTSA/HFIP system proved to be a
237 lot more superior than TfOH/DCE in the COM cyclization (products **2a** and **2'e**). For the 6-*endo-trig*
238 cyclization (products **6a** and **6e/6e'**), TfOH/DCE was slightly inferior to pTSA/HFIP, especially when it
239 came to the formation of Friedel-Crafts type product **6e'** at elevated temperature. Similar
240 catalyst/solvent-reactivity relationship was observed for the interrupted COM products (**4a** and **4d**).
241 Surprisingly, with electron deficient substrates, the COM reactions (**2i** and **2z**) did not work well in all
242 conditions; the interrupted COM substrates actually led to the formation of six-membered ring normal
243 COM products (**4x/2x** and **4y/2y**); while the 6-*endo-trig* reactions (**6x** and **6y**) work well under all
244 conditions. These results once again confirmed the very important role of HFIP solvent and formation
245 of hydrogen bond networks in these Brønsted acid catalyzed reactions.

246

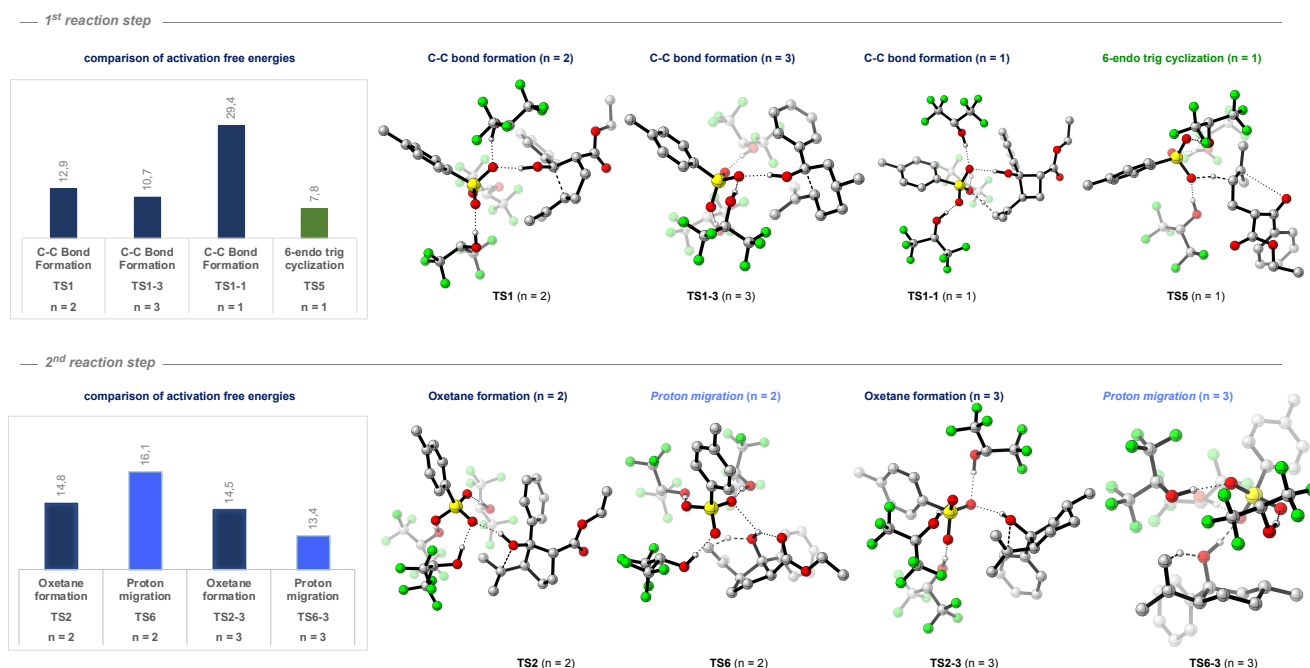
247

required in scarce number of reports for the latter.^{9f, 15b} We therefore carried out computational studies on the COM reaction pathway and all other reaction pathways observed for different chain length of the alkenyl carbon skeleton (Scheme 4). The analysis of the first reaction step showed a distinct effect of the carbon chain length on the activation free energy for C-C bond formation (**TS1**). This step is energetically favored for the hexene (**1**, $n = 2$) and heptene (**3**, $n = 3$) substrates, while being energetically highly unfavorable for the shorter pentene derivative (**5**, $n = 1$) due to the high ring strain of the putative 1-oxo-bicyclo-[2.2.0]-hexane intermediate (**TS1-1**) (Scheme 4, dark blue). Instead, **5** preferentially undergoes a 6-*endo* dig cyclization reaction via **TS5** to give pyrane **6a** (Scheme 4, green). The analysis of similar cyclization pathways for hexene (**1**, $n = 2$) and heptene (**3**, $n = 3$) substrates showed that such cyclization is indeed possible, yet unfavored due to the formation of larger ring systems and transannular interactions within such ring systems.²⁷

a) Analysis of reaction pathways for different side chains



b) Comparison of activation free energy and transition state structures for different chain length for key reaction steps



Scheme 4. Comparison of the influence of the alkenyl chain length on the reaction outcomes.

The second reaction step then rationalizes for the divergent reactivity of the hexene (**1**, $n = 2$) and heptene (**3**, $n = 3$) substrates. Both substrates can potentially undergo a proton migration reaction²⁸ via the bicyclic transition state **TS6**, which results in the product of a classic Ene reaction (**INT4**) via a stepwise reaction mechanism. Following the stepwise Ene reaction, the tricyclic reaction product **6a** (Scheme 4, light blue) is formed, which is often referred to as the product of an interrupted COM reaction. The interruption of the Ene reaction pathway however, allows the formation of the bicyclic oxetane intermediate (**INT2**) via transition state **TS2** that ultimately leads to COM reaction (Scheme 4, dark blue). Thus, the initial steps of a COM reaction can also be regarded as an interrupted stepwise Ene reaction. This pathway is favored only in the case of the hexene derivative **1**, as the formation of bicyclic oxetane intermediate **INT2** is conformationally accessible due to the envelope conformation of 5-membered rings. In the case of heptenes (**3**), this pathway cannot be accessed as the six-membered ring needs to adapt an unfavorable twist boat conformation. Small differences in the energy of transition states that result from conformational restriction of bicyclic transition states and/or intermediates thus open a divergent reactivity that can lead to cyclization, carbonyl olefin metathesis or Ene reaction.

Conclusion

In summary, we report on a combined experimental and computational study on the activation of catalysts by hydrogen bonding interaction. We show that HFIP can act as a hydrogen bond donor to enhance the catalytic efficiency of simple Brønsted acid catalysts by stabilization of all transition states and intermediates along the reaction pathway. This mode of activation could successfully be employed to allow for a novel and practical method for the direct Brønsted acid catalyzed carbonyl-olefin metathesis reaction. Interesting insights into the effect of the alkenyl moiety chain length on the reaction outcomes were also revealed, which give the rationalization for the current ring-size limitation of COM cyclization reaction products. These results will not only advance the catalytic scope of the COM reaction further into homogeneous Brønsted acid catalysis but also pave the way for further investigations and applications of hydrogen bonding network assisted catalysis in organic synthesis.

299 ASSOCIATED CONTENT

300 Supporting Information

301 The Supporting Information is available free of charge: Experimental details and spectroscopic data for
302 all products, full Gaussian reference, Cartesian coordinates, electronic and free energies.

303 AUTHOR INFORMATION

304 Materials and Correspondence

305 *RMK. E-mail: rene.koenigs@rwth-aachen.de

306 *TVN. E-mail: t.v.nguyen@unsw.edu.au

307

308 Author Contributions

309 The manuscript was written through contributions of all authors. TAT carried out all experimental
310 work; TVN and RMK conceived the ideas and designed the project. CP and RMK carried out all
311 computational studies. All authors have given approval to the final version of the manuscript.

312 CONFLICTS OF INTEREST

313 There is no conflicts of interest to declare.

314 ACKNOWLEDGMENTS

315 This work was funded by the Australian Research Council (grant FT180100260 to TVN and
316 DP200100063 to TVN and RMK). CP thanks China Scholarship Council for a PhD scholarship.

317 REFERENCES

318

319 1. Anslyn, E. V.; Dougherty, D. A., In *Modern Physical Organic Chemistry*, University Science Books:
320 California, 2006; pp 145-204.

321 2. Jeffrey, G. A.; Saenger, W., Hydrogen Bonding in Biological Structures. In *Hydrogen Bonding in*
322 *Biological Structures*, Springer: Berlin Heidelberg, 1991; pp 167-422.

323 3. Meeuwissen, J.; Reek, J. N. H., Supramolecular catalysis beyond enzyme mimics. *Nature Chem.*
324 **2010**, 2 (8), 615-621.

325 4. a) Herschlag, D.; Pinney, M. M., Hydrogen Bonds: Simple after All? *Biochemistry* **2018**, 57 (24),
326 3338-3352; b) Karas, L. J.; Wu, C.-H.; Das, R.; Wu, J. I.-C., Hydrogen bond design principles. *WIREs*

327 *Comput. Mol. Sci.* **2020**, *10* (6), e1477; c) Dai, S.; Funk, L.-M.; von Pappenheim, F. R.; Sautner, V.;
328 Paulikat, M.; Schröder, B.; Uranga, J.; Mata, R. A.; Tittmann, K., Low-barrier hydrogen bonds in
329 enzyme cooperativity. *Nature* **2019**, *573* (7775), 609-613.

330 5. a) Schreiner, P. R., Metal-free organocatalysis through explicit hydrogen bonding interactions.
331 *Chem. Soc. Rev.* **2003**, *32* (5), 289-296; b) Knowles, R. R.; Jacobsen, E. N., Attractive noncovalent
332 interactions in asymmetric catalysis: Links between enzymes and small molecule catalysts. *Proc. Natl.*
333 *Acad. Sci. U.S.A.* **2010**, *107* (48), 20678-20685.

334 6. Schreiner, P. R., Cooperativity Tames Reactive Catalysts. *Science* **2010**, *327* (5968), 965-966.

335 7. Colomer, I.; Chamberlain, A. E. R.; Haughey, M. B.; Donohoe, T. J., Hexafluoroisopropanol as a
336 highly versatile solvent. *Nature Rev. Chem.* **2017**, *1* (11), 0088.

337 8. Pozhydaiev, V.; Power, M.; Gandon, V.; Moran, J.; Lebœuf, D., Exploiting
338 hexafluoroisopropanol (HFIP) in Lewis and Brønsted acid-catalyzed reactions. *Chem. Commun.* **2020**,
339 *56* (78), 11548-11564.

340 9. a) Griffith, A. K.; Vanos, C. M.; Lambert, T. H., Organocatalytic Carbonyl-Olefin Metathesis. *J.*
341 *Am. Chem. Soc.* **2012**, *134* (45), 18581-18584; b) Veluru Ramesh, N.; Bah, J.; Franzén, J., Direct
342 Organocatalytic Oxo-Metathesis, a trans-Selective Carbocation-Catalyzed Olefination of Aldehydes.
343 *Eur. J. Org. Chem.* **2015**, *2015* (8), 1834-1839; c) Ludwig, J. R.; Zimmerman, P. M.; Gianino, J. B.;
344 Schindler, C. S., Iron(III)-catalysed carbonyl-olefin metathesis. *Nature* **2016**, *533* (7603), 374-379; d)
345 Ma, L.; Li, W.; Xi, H.; Bai, X.; Ma, E.; Yan, X.; Li, Z., FeCl₃-Catalyzed Ring-Closing Carbonyl-Olefin
346 Metathesis. *Angew. Chem. Int. Ed.* **2016**, *55* (35), 10410-10413; e) Pitzer, L.; Sandfort, F.; Strieth-
347 Kalthoff, F.; Glorius, F., Carbonyl-Olefin Cross-Metathesis Through a Visible-Light-Induced 1,3-Diol
348 Formation and Fragmentation Sequence. *Angew. Chem. Int. Ed.* **2018**, *57* (49), 16219-16223; f)
349 Djurovic, A.; Vayer, M.; Li, Z.; Guillot, R.; Baltaze, J.-P.; Gandon, V.; Bour, C., Synthesis of Medium-
350 Sized Carbocycles by Gallium-Catalyzed Tandem Carbonyl-Olefin Metathesis/Transfer Hydrogenation.
351 *Org. Lett.* **2019**, *21* (19), 8132-8137.

352 10. Albright, H.; Davis, A. J.; Gomez-Lopez, J. L.; Vonesh, H. L.; Quach, P. K.; Lambert, T. H.;
353 Schindler, C. S., Carbonyl-Olefin Metathesis. *Chem. Rev.* **2021**.

354 11. a) Lee, A.-L., Organocatalyzed Carbonyl-Olefin Metathesis. *Angew. Chem. Int. Ed.* **2013**, *52* (17),
355 4524-4525; b) Hennessy, E. T.; Jacobsen, E. N., Organometallic chemistry: A new metathesis. *Nat Chem*
356 **2016**, *8* (8), 741-742; c) Saá, C., Iron(III)-Catalyzed Ring-Closing Carbonyl-Olefin Metathesis. *Angew.*
357 *Chem. Int. Ed.* **2016**, *55* (37), 10960-10961; d) Ludwig, J. R.; Schindler, C. S., Lewis Acid Catalyzed
358 Carbonyl-Olefin Metathesis. *Synlett* **2017**, *28* (13), 1501-1509; e) Becker, M. R.; Watson, R. B.;
359 Schindler, C. S., Beyond olefins: new metathesis directions for synthesis. *Chem. Soc. Rev.* **2018**, *47* (21),
360 7867-7881; f) Ravindar, L.; Lekkala, R.; Rakesh, K. P.; Asiri, A. M.; Marwani, H. M.; Qin, H.-L., Carbonyl-

olefin metathesis: a key review. *Organic Chemistry Frontiers* **2018**, 5 (8), 1381-1391; g) Das, A.; Sarkar, S.; Chakraborty, B.; Kar, A.; Jana, U., Catalytic Alkyne/Alkene-Carbonyl Metathesis: Towards the Development of Green Organic Synthesis. *Current Green Chemistry* **2020**, 7 (1), 5-39.

12. a) Ludwig, J. R.; Phan, S.; McAtee, C. C.; Zimmerman, P. M.; Devery, J. J.; Schindler, C. S., Mechanistic Investigations of the Iron(III)-Catalyzed Carbonyl-Olefin Metathesis Reaction. *J. Am. Chem. Soc.* **2017**, 139 (31), 10832-10842; b) McAtee, C. C.; Riehl, P. S.; Schindler, C. S., Polycyclic Aromatic Hydrocarbons via Iron(III)-Catalyzed Carbonyl-Olefin Metathesis. *J. Am. Chem. Soc.* **2017**, 139 (8), 2960-2963; c) Groso, E. J.; Golonka, A. N.; Harding, R. A.; Alexander, B. W.; Sodano, T. M.; Schindler, C. S., 3-Aryl-2,5-Dihydropyrroles via Catalytic Carbonyl-Olefin Metathesis. *ACS Catal.* **2018**, (8), 2006-2011; d) Groso, E. J.; Golonka, A. N.; Harding, R. A.; Alexander, B. W.; Sodano, T. M.; Schindler, C. S., 3-Aryl-2,5-Dihydropyrroles via Catalytic Carbonyl-Olefin Metathesis. *ACS Catal.* **2018**, 8 (3), 2006-2011; e) Albright, H.; Riehl, P. S.; McAtee, C. C.; Reid, J. P.; Ludwig, J. R.; Karp, L. A.; Zimmerman, P. M.; Sigman, M. S.; Schindler, C. S., Catalytic Carbonyl-Olefin Metathesis of Aliphatic Ketones: Iron(III) Homo-Dimers as Lewis Acidic Superelectrophiles. *J. Am. Chem. Soc.* **2019**, 141 (4), 1690-1700; f) Riehl, P. S.; Nasrallah, D. J.; Schindler, C. S., Catalytic, transannular carbonyl-olefin metathesis reactions. *Chem. Sci.* **2019**, 10 (44), 10267-10274; g) Rykaczewski, K. A.; Groso, E. J.; Vonesh, H. L.; Gaviria, M. A.; Richardson, A. D.; Zehnder, T. E.; Schindler, C. S., Tetrahydropyridines via FeCl₃-Catalyzed Carbonyl-Olefin Metathesis. *Org. Lett.* **2020**, 22 (7), 2844-2848.

13. Albright, H.; Vonesh, H. L.; Becker, M. R.; Alexander, B. W.; Ludwig, J. R.; Wiscons, R. A.; Schindler, C. S., GaCl₃-Catalyzed Ring-Opening Carbonyl-Olefin Metathesis. *Org. Lett.* **2018**, 20 (16), 4954-4958.

14. Wang, R.; Chen, Y.; Shu, M.; Zhao, W.; Tao, M.; Du, C.; Fu, X.; Li, A.; Lin, Z., AuCl₃-Catalyzed Ring-Closing Carbonyl-Olefin Metathesis. *Chem. Eur. J.* **2020**, 26 (9), 1941-1946.

15. a) Albright, H.; Vonesh, H. L.; Schindler, C. S., Superelectrophilic Fe(III)-Ion Pairs as Stronger Lewis Acid Catalysts for (E)-Selective Intermolecular Carbonyl-Olefin Metathesis. *Org. Lett.* **2020**, 22 (8), 3155-3160; b) Davis, A. J.; Watson, R. B.; Nasrallah, D. J.; Gomez-Lopez, J. L.; Schindler, C. S., Superelectrophilic aluminium(iii)-ion pairs promote a distinct reaction path for carbonyl-olefin ring-closing metathesis. *Nature Catal.* **2020**, 3 (10), 787-796.

16. a) Hong, X.; Liang, Y.; Griffith, A. K.; Lambert, T. H.; Houk, K. N., Distortion-accelerated cycloadditions and strain-release-promoted cycloreversions in the organocatalytic carbonyl-olefin metathesis. *Chem. Sci.* **2014**, 5 (2), 471-475; b) Lambert, T. H., Development of a Hydrazine-Catalyzed Carbonyl-Olefin Metathesis Reaction. *Synlett* **2019**, 30 (17), 1954-1965; c) Zhang, Y.; Jermaks, J.; MacMillan, S. N.; Lambert, T. H., Synthesis of 2H-Chromenes via Hydrazine-Catalyzed Ring-Closing Carbonyl-Olefin Metathesis. *ACS Catal.* **2019**, 9 (10), 9259-9264; d) Jermaks, J.; Quach, P. K.; Seibel, Z.

395 M.; Pomarole, J.; Lambert, T. H., Ring-opening carbonyl–olefin metathesis of norbornenes. *Chem. Sci.*
396 **2020**, *11* (30), 7884-7895; e) Zhang, Y.; Sim, J. H.; MacMillan, S. N.; Lambert, T. H., Synthesis of 1,2-
397 Dihydroquinolines via Hydrazine-Catalyzed Ring-Closing Carbonyl–Olefin Metathesis. *Org. Lett.* **2020**,
398 *22* (15), 6026-6030.

399 17. Ni, S.; Franzén, J., Carbocation catalysed ring closing aldehyde–olefin metathesis. *Chem.*
400 *Commun.* **2018**, *54* (92), 12982-12985.

401 18. Tran, U. P. N.; Oss, G.; Pace, D. P.; Ho, J.; Nguyen, T. V., Tropylium-promoted carbonyl–olefin
402 metathesis reactions. *Chem. Sci.* **2018**, *9*, 5145-5151.

403 19. a) Oss, G.; Nguyen, T. V., Iodonium-Catalyzed Carbonyl–Olefin Metathesis Reactions. *Synlett*
404 **2019**, *30* (17), 1966-1970; b) Tran, U. P. N.; Oss, G.; Breugst, M.; Detmar, E.; Pace, D. P.; Liyanto, K.;
405 Nguyen, T. V., Carbonyl–Olefin Metathesis Catalyzed by Molecular Iodine. *ACS Catal.* **2019**, *9* (2), 912-
406 919.

407 20. a) Roth, D.; Stirn, J.; Stephan, D. W.; Greb, L., Lewis Superacidic Catecholato Phosphonium
408 Ions: Phosphorus–Ligand Cooperative C–H Bond Activation. *J. Am. Chem. Soc.* **2021**, *143* (38), 15845-
409 15851; b) Thorwart, T.; Roth, D.; Greb, L., Bis(pertrifluoromethylcatecholato)silane: Extreme Lewis
410 Acidity Broadens the Catalytic Portfolio of Silicon. *Chemistry – A European Journal* **2021**, *27* (40),
411 10422-10427.

412 21. Catti, L.; Tiefenbacher, K., Brønsted Acid-Catalyzed Carbonyl–Olefin Metathesis inside a Self-
413 Assembled Supramolecular Host. *Angew. Chem. Int. Ed.* **2018**, *57* (44), 14589-14592.

414 22. Rivero-Crespo, M. Á.; Tejeda-Serrano, M.; Pérez-Sánchez, H.; Cerón-Carrasco, J. P.; Leyva-
415 Pérez, A., Intermolecular Carbonyl–olefin Metathesis with Vinyl Ethers Catalyzed by Homogeneous and
416 Solid Acids in Flow. *Angew. Chem. Int. Ed.* **2020**, *59* (10), 3846-3849.

417 23. a) Ludwig, J. R.; Watson, R. B.; Nasrallah, D. J.; Gianino, J. B.; Zimmerman, P. M.; Wiscons, R.
418 A.; Schindler, C. S., Interrupted carbonyl–olefin metathesis via oxygen atom transfer. *Science* **2018**, *361*
419 (6409), 1363-1369; b) Malakar, T.; Zimmerman, P. M., Brønsted-Acid-Catalyzed Intramolecular
420 Carbonyl–Olefin Reactions: Interrupted Metathesis vs Carbonyl–Ene Reaction. *J. Org. Chem.* **2021**, *86*
421 (3), 3008-3016.

422 24. *See the experimental Supporting Information for more details.*

423 25. Li, G.-X.; Morales-Rivera, C. A.; Gao, F.; Wang, Y.; He, G.; Liu, P.; Chen, G., A unified
424 photoredox-catalysis strategy for C(sp³)–H hydroxylation and amidation using hypervalent iodine.
425 *Chem. Sci.* **2017**, *8* (10), 7180-7185.

426 26. Watson, R. B.; Schindler, C. S., Iron-Catalyzed Synthesis of Tetrahydronaphthalenes via 3,4-
427 Dihydro-2H-pyran Intermediates. *Org. Lett.* **2018**, *20* (1), 68-71.

428 27. *See the computational Supporting Information for more details.*

429 28. Jana, S.; Yang, Z.; Li, F.; Empel, C.; Ho, J.; Koenigs, R. M., Photoinduced Proton-Transfer
430 Reactions for Mild O-H Functionalization of Unreactive Alcohols. *Angew. Chem. Int. Ed.* **2020**, *59* (14),
431 5562-5566.

432